



Removal of indigo carmine from aqueous solution by microwave-treated activated carbon from peanut shell

Jixiang Zhang^{a,*}, Qiuxiang Zhou^a, Lailiang Ou^b

^aDepartment of Chemistry, Langfang Teachers' College, Langfang, Hebei 065000, China, Tel. +86 316 2188377;

Fax: +86 316 2188416; email: zhangjixiang1973@163.com (J. Zhang)

^bKey Laboratory of Bioactive Materials of Ministry of Education, Institute of Molecular Biology, Nankai University, Tianjin 300071, China

Received 27 March 2014; Accepted 14 September 2014

ABSTRACT

Activated carbon (AC) prepared from peanut shell (PS) with microwave treatment was used to remove indigo carmine (IC) from aqueous solution in this study. PS and AC were examined by pore structural analysis, scanning electron microscopy, and elemental analysis. Effect of initial dye concentration, contact time, pH, and temperature on IC removal was investigated by batch experiments. The adsorption capacity increased with the increase of initial concentration, and decreased with increasing pH. Higher temperatures were favorable for the adsorption. The adsorption equilibrium could be reached within 90 min for all studied concentrations. The results showed that the Langmuir isotherm model had a good fit for the equilibrium data. Kinetic studies revealed that the adsorption followed the pseudo-second-order kinetic model. Thermodynamic studies indicated that the adsorption was a spontaneous, endothermic process.

Keywords: Activated carbon; Adsorption; Indigo carmine; Microwave; Peanut shell

1. Introduction

In recent years, a large amount of wastewater containing the highly visible synthetic dyes was discharged to aquatic environment due to the rapid development of the modern textile industry. Some of these dyes are toxic and can cause serious threat to the environment. Over the past few decades, discharging of dyes wastewater without any treatment into water system has led to serious environmental problem in China [1]. Indigo carmine (IC), a water-soluble disulfonate derivative, has a wide range of applications as a coloring agent in many fields. It has been used as

textile dyeing agent, an additive in pharmaceutical, and so on. IC is also applied in analytical chemistry and biological detection [2]. Although its application covers a broad range, the usage of IC is restricted strictly. It is considered to be a toxic indigoid dye, and excessive consumption and direct touch of IC can irritate the eyes and skin of human beings. The application of IC can also cause reproductive, developmental, and acute toxicity. The investigation of the removal of IC from aqueous solution should be useful for further research and practical applications in wastewater treatment. Recently, several studies have been reported to remove IC from wastewater [3–5].

The conventional methods for treatment of wastewater containing dye are chemical oxidation [6],

*Corresponding author.

coagulation/flocculation [7], filtration [8], membrane [9], and adsorption [10]. Among the above-mentioned methods, adsorption is widely applied as a simple and efficient technique. Recently, a variety of adsorbents, such as low-cost nature inorganic minerals or industrial and agricultural waste, have been used for treatment of dyes wastewater over a period of time [11–17].

As an agricultural by-product, peanut shell (PS) is mainly used as fuel, feed, or discarded as waste. It is meaningful to convert the agricultural waste to useful and value-added products. Several studies have been conducted to prepare activated carbon (AC) from PS by chemical modification. The AC adsorbents from PS demonstrate good adsorption capacity for certain metal ions and organic compounds [18,19]. In this study, AC was prepared from PS using H_3PO_4 as an activating agent with microwave treatment. Microwave radiation supplies energy to the carbon skeleton at the molecular level [20,21]. In this study, the effect of initial concentration, time, pH, and temperature on the adsorption of IC onto AC from aqueous solution was systematically studied. Adsorption thermodynamics, isotherm, and kinetics for the adsorption process were also discussed.

2. Materials and methods

2.1. Materials

All reagents used were of analytical grade. Double-distilled water was used to prepare experimental solutions. Eighty-five percent (wt) phosphoric acid (H_3PO_4) was provided by Shanghai Hushi Chemical Reagent Co., Ltd. The molecular formula of IC (J&K Scientific Co., Ltd, 99% purity) is $\text{C}_{16}\text{H}_8\text{N}_2\text{Na}_2\text{O}_8\text{S}_2$. The molecular structure of IC is shown in Fig. 1. PS, used in the study, was obtained from the suburban area of Langfang, China. The collected sample was extensively washed to remove the dirt and dust with tap water for 30 min and rinsed with deionized water for 10 min, and then dried at 80°C to a constant weight in a vacuum-drying oven. Dried PS was ground and the powder was sieved to 80–100 meshes (0.177–0.149 mm).

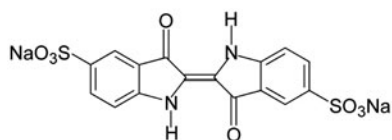


Fig. 1. Chemical structure of IC.

2.2. Preparation and characterization of AC

AC from PS treated from microwave was prepared according to the following procedure. The PS powder was soaked in 50% H_3PO_4 solution in a mass ratio of 1:3 (powder: H_3PO_4) for 4 h in an evaporating dish. The dish containing the sample was fitted into a household-type microwave oven (Galanz, G80W23CSP-2, 800W, China). The oven has a power controller to select different power levels and a timer for various exposure times at a set microwave power level. The dish was installed on the bottom of the microwave oven, where the PS powder was exposed to microwave irradiation. The sample was subjected to microwave treatment for 15 min, and the input power was set at 320 W and the microwave frequency was 2.45 GHz. The activated product was washed repeatedly with 0.1 M NaOH solution and distilled water until the residual solution reached neutral. In the end, the dried AC adsorbent was dried at 70°C for 6 h under vacuum.

2.3. Characterization

The product, AC, and raw material, PS, were characterized by SEM (KYKY-2800B, SEM KYKY Technology Development Ltd) to search for the changes in micromorphology. The surface area and pore structural analysis were implemented by surface area analyzer (Micromeritics Instrument Corporation, ASAP 2010-M, USA). The surface area (S_{BET}) was calculated from N_2 adsorption isotherm based on the BET method. The total pore volume (V_T) was estimated from nitrogen adsorption at a relative pressure of 0.99. The micropore volume (V_{micro}) and mean pore width (nm) were calculated by Dubinin–Radushkevich (D–R) method. The percentage contents of C, H, and O and N elements of AC and PS were measured using a CE-440 elemental analyzer (Exeter Analytical, Inc. USA).

2.4. Preparation and analysis of dye solutions

The dye solutions used in the study were made by dilution of a stock solution of IC with the concentration of 1 g/L with distilled water. The concentration of IC solution in the adsorption experiment was determined by spectrophotometry. The absorbance of the dye solution in the supernatant was measured at the maximum absorbance wavelength of IC (608 nm) using a UV–vis Spectrophotometer (UV-2550, Shimadzu, Japan) and the dye concentration was calculated from the linear regression equation of the calibration curve.

2.5. Adsorption experiments

The effects of initial IC concentration, time, and temperature on the adsorption of IC by AC were conducted and the adsorption process was analyzed in adsorption isotherms, thermodynamic, and kinetics. In all batch experiments, 50 mL of IC solution and 0.20 g of AC adsorbent (4 g/L) in Erlenmeyer flasks (250 mL) were employed and the adsorption was conducted in a thermostat water bath shaker (THZ-82A, Ronghua, China) with an agitation speed of 110 rpm at a given temperature with an accuracy of 0.1 °C. The Erlenmeyer flasks were taken out from the oscillator at a given time and the mixture was centrifuged to separate the supernatant of IC from the AC adsorbents at 4,000 rpm for 10 min. The equilibrium concentration of the supernatant was calculated from the linear regression equation by measuring the absorbance of the solution at the wavelength 608 nm. The effect of initial concentration on the adsorption was performed by varying concentrations (100–500 mg/L) at 25 °C. For the study of time effect, the mixtures of IC solution and AC adsorbent were agitated at 25 °C and the residual dye concentration was analyzed at the predetermined time until the adsorption equilibrium was reached. For the effect of temperature on the adsorption, experiments were carried out by increasing the temperature from 25 to 45 °C with an interval of 5 °C in the adsorption equilibrium state. All data were the average from experiments duplicated under identical conditions. The equilibrium adsorption capacity of AC for IC, q_e (mg/g), was calculated by the following relationship:

$$q_e = \frac{(C_i - C_e)V}{W} \quad (1)$$

where C_i , C_e , and V are the initial and equilibrium concentrations (mg/L) and the volume (L) of IC solution, respectively, W is the mass (g) of the adsorbent.

2.6. Desorption experiments

Desorption experiments were carried out immediately following the completion of the adsorption experiments performed using an initial concentration of IC 500 mg/L. After adsorption equilibrium was reached, the adsorbed AC was separated from the supernatant by centrifugation and decanting the supernatant carefully. Then, 50 mL of double-distilled water used to transfer the adsorbed AC from the centrifugal tube to an Erlenmeyer flask. The mixture was agitated at a shaking speed of 110 rpm at 25 °C for 4 h.

The desorbed IC in the solution was separated and analyzed using the same procedure described in the adsorption section. Similar experiments were carried out with 0.1 mol/L HCl, 0.1 mol/L NaOH, and 50% ethanol solutions. Desorption was also investigated using boiling double-distilled water for the same time without agitation.

3. Results and discussion

3.1. Characterization

The SEM images of AC and PS are shown in Fig. 2. It can be seen that the powder of PS presents irregular thin-film forms at a magnification of 500 times. Some of them look like single-layer thin films, and some seem to be multi-layer films stocked together. However, AC demonstrates a bumpy appearance of the surface and porous structure and displays more applicable surface properties than the raw sample as an adsorbent.

The results of elemental analysis and surface properties for AC and PS are given in Table 1. It can be seen that PS is very similar to wood, which has an elemental composition of about 50% carbon, 6% hydrogen, and 1% nitrogen. The mass percentage of hydrogen and nitrogen of AC decreased compared to PS. It can be concluded that hydrogen and nitrogen have been released from PS in the form of water vapor and nitrogen oxide under the action of phosphoric acid and high-temperature microwave treatment. The results of specific surface area and porosity show that AC presents better surface properties and ability to remove IC from aqueous solutions than PS. The specific surface area and the microporous volume of AC were both increased more than 200 times that of PS, respectively.

3.2. Effect of initial dye concentration

The initial concentration is an important factor affecting IC adsorption onto AC. When using carbon materials as adsorbents, the adsorption capacity generally increases with an increase in initial concentration. The effect of initial concentration on IC removal by AC is shown in Fig. 3. The result clearly reflected that the adsorption capacity increased with the increase in the initial concentration. The equilibrium adsorption capacity of AC for IC, q_e , increases from 24.35 to 112.60 mg/g corresponding to initial concentration of 100 and 500 mg/L. While the percentage of IC removal was 97.38% for 100 mg/L, it was 91.08% for 500 mg/L. The percentage of IC removal is still greater than 90% when the initial concentration is as

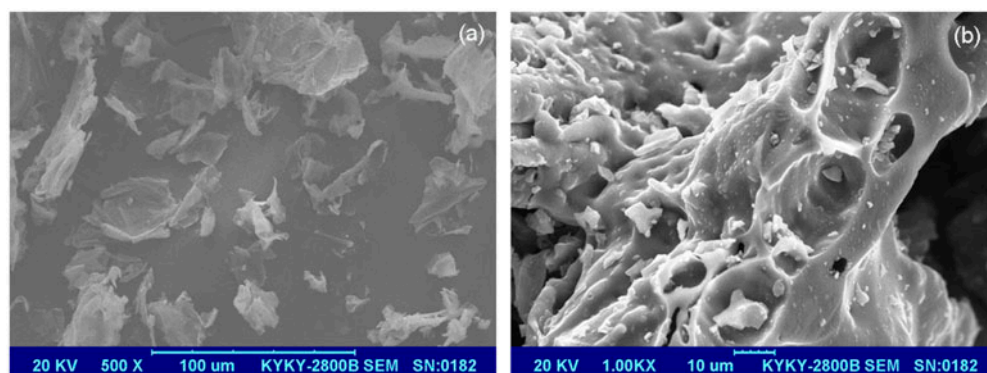


Fig. 2. Scanning electron micrographs: (a) PS and (b) AC.

Table 1
Elemental analysis and surface properties for PS and AC

Sample	C (wt%)	H (wt%)	N (wt%)	O (wt%)	S_g (BET) (m ² /g)	V_T ($P/P_0 = 0.99$) (cm ³ /g)	V_{micro} (cm ³ /g)	Mean pore width (nm)
PS	44.46	5.74	1.77	46.92	3.6	0.033	0.0013	18.3
AC	60.90	3.42	0.40	34.65	763.4	0.398	0.344	1.04

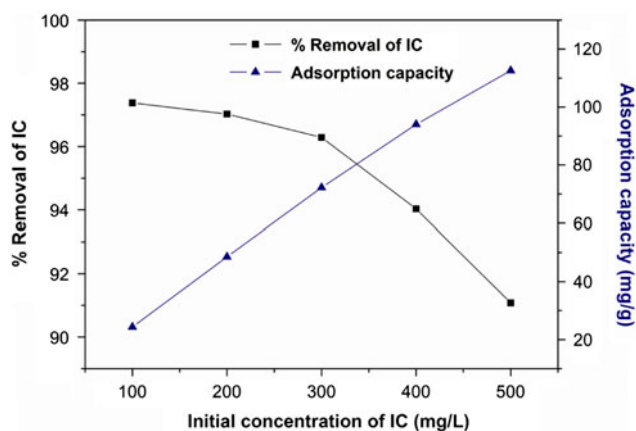


Fig. 3. Effect of initial dye concentration on the IC removal (the initial dye concentration = 100–500 mg/L, AC dose = 4 g/L, and time = 90 min).

high as 500 mg/L, thus the adsorption capacity is roughly proportional to the initial concentration.

The initial concentration provides the necessary driving force to overcome the mass transfer resistance of IC between liquid phase and the solid phase. The concentration gradient of solute between the solution and the adsorbent increases with increasing dye concentration, which makes the mass transfer process strengthened from the bulk of the IC solution to the surface and pores of AC [22]. The increase in the

initial concentration of IC also enhances the interaction between IC and AC, and the adsorption uptake of IC onto AC. Therefore, the adsorption capacity is enhanced with the increase in initial concentration of IC.

3.3. Effect of contact time

Experiments were performed to study the effect of contact time on the removal of IC by AC. The plot of % IC removal vs. time is shown in Fig. 4. There was a general increase in the % adsorption of IC with time. As a result, shown in the figure, the adsorption was fast in the initial stage, and then slowed down at later stages. For the solutions with the concentration of 100 and 200 mg/L, the adsorption reached equilibrium only 40 min later. For the other three IC solutions of different concentrations, the adsorption slowed down after 40 min and gradually approached equilibrium after approximately 80 min. This shows that the adsorption capacity increases with contact time and the required time to reach adsorption equilibrium gets longer with increasing the initial dye concentration.

The adsorption of IC onto AC reaches a pseudo-equilibrium state with the increasing time. The adsorption capacity increases with time and, at some point in time, reaches a constant value where the dye amount adsorbed onto AC is equal to the amount desorbed from AC. With the initial concentration

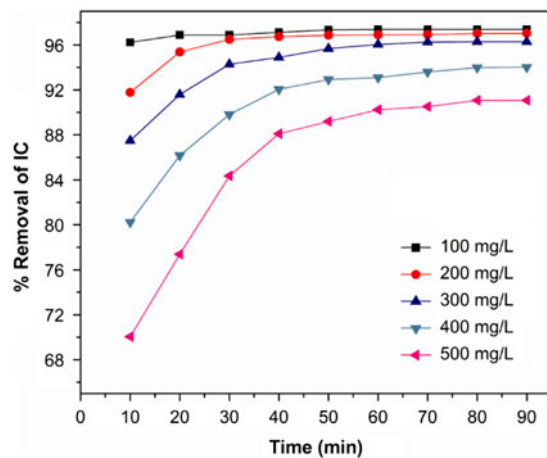


Fig. 4. Effect of contact time on the IC removal (the initial dye concentration = 100–500 mg/L, AC dose = 4 g/L, and time = 90 min).

increasing, the driving force of IC to overcome the mass transfer resistance at the liquid–solid interface also increases, so that more adsorption sites could be occupied and the adsorption capacity is enhanced. However, with the increase in initial concentrations, the competition for the adsorption sites also increases and the required contact time to reach adsorption equilibrium is increased accordingly.

3.4. Effect of pH

The point of zero charge (pH_{PZC}) of AC was determined to better understand the adsorption mechanism. The adsorption is favorable for cations at pH higher than pH_{PZC} , while the adsorption is favorable for anions at pH lower than pH_{PZC} . The pH of point zero charge of AC, as determined by the method proposed by Wang and Reardon [23], was equal to 3.2. The effect of pH on the adsorption of IC onto AC at 25°C with dye concentration of 500 mg/L is shown in Fig. 5. It can be seen that the adsorption capacity decreases with the increasing pH. The protonation of AC occurs at low pH values, which results in the strong electrostatic attraction between the positively charged AC and the anionic dye molecules. With the increase in pH, the AC tends to deprotonate and the adsorption decreases due to the electrostatic repulsion between the AC and the IC dye molecules.

3.5. Effect of temperature

The effect of temperature on the removal of IC by AC was studied using batch experiments. The plot of % IC removal vs. temperature is given in Fig. 6.

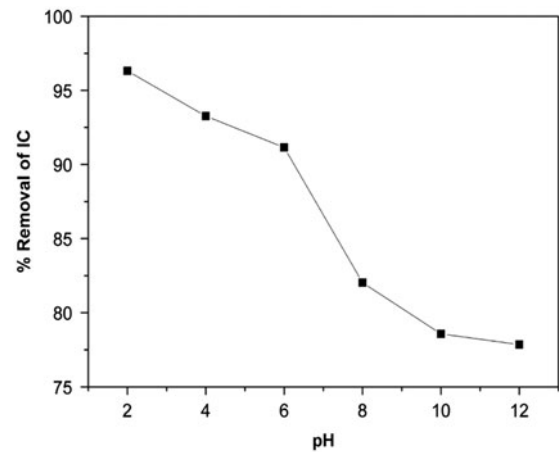


Fig. 5. Effect of pH on the IC removal (the initial dye concentration = 500 mg/L, AC dose = 4 g/L, and time = 90 min).

It was found that the maximum removal of IC was obtained at 45°C. The percentage removal of IC increased for IC solutions of different concentrations with increasing temperature. In addition, the higher the initial concentration, the greater the percentage of IC removal improved with an increase in temperature. The temperature showed little impact on IC solutions with low concentration relative to IC solutions of high concentrations.

The increase in dye adsorption with increasing temperature might be due to an increase in the number of active surfaces available for adsorption with an increase in temperature and due to an enhanced rate of intraparticle diffusion of the adsorbate, as diffusion is an endothermic process [24]. The result indicated

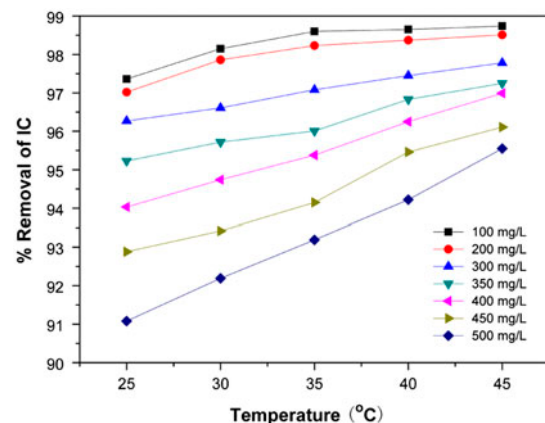


Fig. 6. Effect of temperature on the IC removal (the initial dye concentration = 100–500 mg/L, AC dose = 4 g/L, and time = 90 min).

that the adsorption of IC by AC prepared from PS might be an endothermic process. Similar results of dye adsorption using agricultural wastes as adsorbents have been presented in several reports [10,16,19].

3.6. Adsorption thermodynamics

Thermodynamics studies were conducted for a better understanding of the effect of temperature on adsorption of IC by AC. Thermodynamic parameters in the IC adsorption process can be determined from the following relations:

$$K_c = \frac{C_{Ac}}{C_e} \quad (2)$$

where K_c , C_{Ac} , and C_e are the equilibrium constant, the mass of IC adsorbed onto AC per liter of the solution at equilibrium (mg/L), and equilibrium concentrations of IC remaining in the solution (mg/L), respectively.

$$\Delta G^\circ = -RT \ln K_c \quad (3)$$

The change in Gibbs free energy (ΔG°), kJ/mol, can be calculated from the above equation, where R is the gas constant (8.314 J/mol/K) and T is the absolute temperature (K).

$$\ln K_c = \frac{\Delta S^\circ}{R} - \frac{\Delta H^\circ}{RT} \quad (4)$$

The enthalpy change (ΔH° , kJ/mol) and entropy change (ΔS° , J/mol K) are computed using the above equations. The plots of $\ln K_c$ vs. $1/T$ under five different temperatures are shown in Fig. 7. ΔH° and ΔS° can be calculated from the slope and the intercept by linear regression analysis. The values of thermodynamic parameters are shown in Table 2. It can be seen that the values of ΔG° from 25 to 45°C are negative, which indicates the adsorption process is spontaneous. Moreover, the values of ΔG° decrease with increasing temperature indicating that the adsorption becomes more feasible at high temperatures. However, the values of ΔG° increase with an increase in the initial concentration. The positive values of ΔH° suggest that the adsorption process is endothermic in nature. The positive values of ΔS° reflect the high affinity of IC onto AC and the increase in randomness at the solid–solution interface.

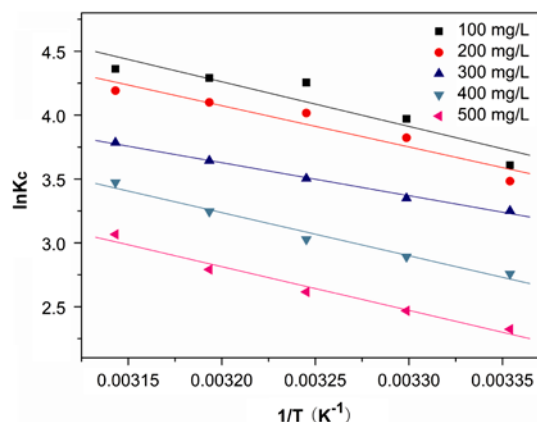


Fig. 7. Thermodynamic study.

3.7. Adsorption isotherms

A study on adsorption isotherms is necessary to further understand the surface properties of AC and the interaction between the AC and IC. The maximum adsorption capacity can be calculated through adsorption isotherm. Two of the most frequently used isotherms, Langmuir and Freundlich isotherm, were used to explore the adsorption mechanism in the study.

The Langmuir isotherm developed by Irving Langmuir is the model which is based on monolayer adsorption. It assumes a homogenous adsorption surface with binding sites having equal energies. The linear form of Langmuir equation is expressed as:

$$\frac{1}{q_e} = \frac{1}{q_m} + \frac{1}{K_L q_m C_e} \quad (5)$$

where q_e is the amount of dye adsorbed per unit mass of adsorbent at equilibrium (mg/g), C_e is the equilibrium concentration of solution after adsorption (mg/L), K_L is the Langmuir constants (L/mg), and q_m is the maximum adsorption capacity (mg/g). The values of q_m and K_L can be calculated from the intercept and the slope of the plot of $1/q_e$ vs. $1/C_e$ by linear regression analysis.

The Freundlich isotherm model developed by Freundlich and Küster is based on the assumption of heterogeneous adsorption surface and existence of interaction among adsorbed molecules. The Freundlich isotherm equation is expressed as:

$$\log q_e = \log K_F + \frac{1}{n} \log C_e \quad (6)$$

Table 2
Thermodynamic parameters for the adsorption of IC onto AC

Initial IC concentration (mg/L)	ΔH° (kJ/mol)	ΔS° (J/mol K)	R^2	ΔG° (kJ/mol)				
				25°C	30°C	35°C	40°C	45°C
100	29.04	128.34	0.8738	-8.94	-10.01	-10.90	-11.17	-11.54
200	26.87	119.87	0.9193	-8.63	-9.64	-10.29	-10.68	-11.09
300	21.46	98.85	0.9940	-8.06	-8.44	-8.98	-9.49	-10.01
400	28.09	116.81	0.9698	-6.83	-7.29	-7.76	-8.45	-9.19
500	28.46	114.46	0.9739	-5.76	-6.22	-6.70	-7.27	-8.11

where K_F and n are Freundlich constants reflecting adsorption capacity and intensity of adsorption, respectively. The values of K_F and n can be obtained from the intercept and the slope of the plot of $\log q_e$ vs. $\log C_e$ by linear regression analysis.

The parameters q_m , K_L , K_F , n , and R^2 (correlation coefficients), associated with Langmuir and Freundlich isotherms for the adsorption of IC onto AC, are listed in Table 3. The graphical presentations for Langmuir and Freundlich adsorption isotherms are presented in Fig. 8. It can be seen that the values of correlation coefficient (R^2) of Langmuir are closer to unity than those of Freundlich for all studied temperatures, as implies that the Langmuir isotherm describes the adsorption process better than the Freundlich isotherm. This result suggests the homogeneous feature of the surface of AC, and IC molecules tend to form a monolayer on the surface of AC.

The dimensionless equilibrium parameter R_L defined by Hall et al. can be used to reveal the feasibility of the adsorption process. This parameter determined from the equation is expressed as:

$$R_L = \frac{1}{(1 + K_L C_i)} \quad (7)$$

where K_L and C_i are the same as mentioned above. The adsorption process would be unfavorable ($R_L > 1$),

linear ($R_L = 1$), favorable ($0 < R_L < 1$), or irreversible ($R_L = 0$). The values of R_L are presented in Table 3. The values of R_L (0.012–0.126) for the studied temperatures indicate that the adsorption of IC onto AC is favorable.

3.8. Adsorption kinetics

In order to identify the adsorption mechanism, the pseudo-second-order and intraparticle diffusion kinetic equations were used to test the experimental data. The pseudo-second-order kinetic equation is given by:

$$\frac{t}{q_t} = \frac{1}{k_2 q_e^2} + \frac{1}{q_e} t \quad (8)$$

where k_2 is the pseudo-second-order kinetic constant (g/mg min) and other parameters in the relationship are the same as above. The parameters, k_2 , q_e , and R^2 were determined from the plots of t/q_t vs. t by linear regression analysis and are listed in Table 4.

The intraparticle diffusion model is given by:

$$q_t = k_i t^{1/2} + C_i \quad (9)$$

where k_i (mg/g min^{0.5}) is the intraparticle diffusion rate constant and C_i is the thickness of the boundary

Table 3
Parameters of Langmuir's and Freundlich's equations

Temperature (°C)	Langmuir				Freundlich		
	K_L (L/mg)	q_m (mg/g)	R_L	R^2	K_F	n	R^2
25	0.0691	159.49	0.028–0.126	0.9973	16.8795	1.8682	0.9498
30	0.1184	137.74	0.017–0.078	0.9970	20.9021	2.0291	0.9612
35	0.1703	128.04	0.012–0.055	0.9986	23.8139	2.1067	0.9694
40	0.1623	137.93	0.012–0.058	0.9986	24.1107	1.9914	0.9678
45	0.1575	149.70	0.013–0.060	0.9989	24.3759	1.8401	0.9742

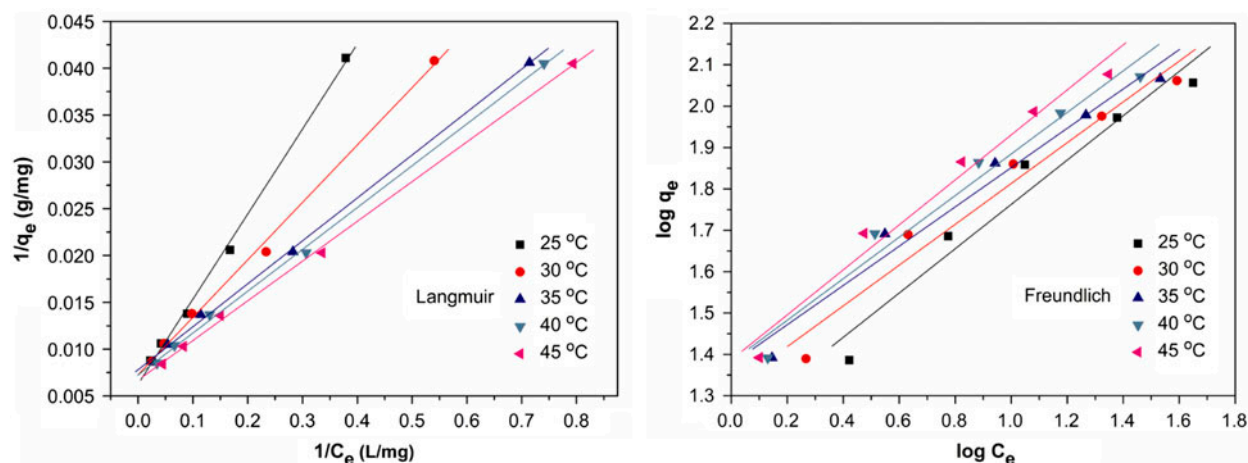


Fig. 8. Langmuir and Freundlich adsorption isotherms for IC-AC system.

layer. The parameters, k_i and C_i , and R^2 were determined from the plots of q_t vs. $t^{1/2}$ by linear regression analysis and are listed in Table 4. The graphical presentations for pseudo-second-order and intraparticle diffusion kinetic models are shown in Fig. 9.

It can be concluded that the kinetic data are perfectly fitted by the pseudo-second-order model with high values of correlation coefficients ($R^2 > 0.999$) in the study. The calculated values of equilibrium adsorption capacity (q_e) are fairly consistent with the experimental values ($q_{e,exp}$). These results show that the adsorption of IC onto AC conforms to the pseudo-second-order kinetic model.

The values of correlation coefficients from intraparticle diffusion model are <0.86 for all studied concentrations. These results show that the IC adsorption onto AC poorly obeys the intraparticle diffusion kinetic model. Moreover, the plot did not pass through the origin implying that the intraparticle diffusion was not the rate-controlling factor. Although intraparticle diffusion model was not fitted well to the kinetic data in the whole adsorption process, there are

two distinct linear trends during the first rapid adsorption phase and the following slow adsorption phase. The rapid adsorption is due to the mass transfer from the IC solution to the external surface of AC, as is followed by a slower phase of intra-particle diffusion [25]. Therefore, both pseudo-second-order and intraparticle diffusion models were involved in the adsorption process of IC onto AC.

3.9. Desorption studies

Desorption studies can be used to elucidate the mechanism of an adsorption process and explore the possibility of recovering the adsorbent and adsorbed adsorbate. Experimental results show that no desorption happens after the loaded adsorbent was agitated in 0.1 mol/L HCl and 0.1 mol/L NaOH solutions at 25°C for 4 h. The desorption percentages are 3.1, 6.8, and 19.7% in double-distilled water, boiling distilled water, 50% ethanol solution, respectively. The result implies that adsorption of IC dye molecules onto the AC is mainly via physical interaction. Desorption increase in

Table 4
Adsorption kinetic constants of and correlation coefficients associated with the pseudo-second-order and intraparticle diffusion equations

Initial IC concentration (mg/L)	Pseudo-second-order				Intraparticle diffusion		
	k_2 (g/mg min)	q_e (mg/g)	$q_{e,exp}$ (mg/g)	R^2	K_i (mg/g min ^{0.5})	C_i	R^2
100	0.2484	24.40	24.34	1.0000	0.042	23.99	0.8398
200	0.0446	48.85	48.52	1.0000	0.325	45.86	0.6483
300	0.0111	73.42	72.22	1.0000	0.951	64.28	0.8165
400	0.0048	96.52	94.03	1.0000	2.025	76.92	0.8448
500	0.0021	119.90	113.85	0.9997	4.032	79.87	0.8572

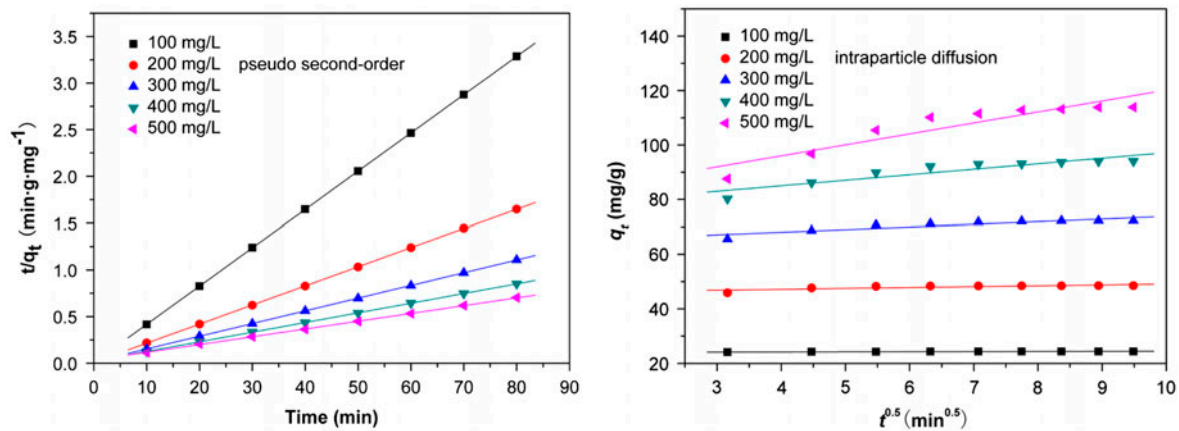


Fig. 9. Pseudo-second-order and intraparticle diffusion models for IC-AC system at 25°C.

higher temperature is due to the acceleration of mobility of IC molecules. ACs can strongly adsorb ethanol via specific interactions between the carbon material and ethanol [26]. Therefore, desorption occurred in the presence of competition from ethanol molecules. The results indicated that recovery and reuse of spent AC may be difficult. As a product from agriculture waste, the spent AC can be used as fuel and the resulting bottom ash can be used for building materials.

4. Conclusion

The AC prepared from PS was used as an adsorbent for the removal of IC from aqueous solution in this study. The increase in initial dye concentration enhances the interaction between IC and AC which results in the increase of adsorption capacity. The increase in solution pH decreases the removal efficiency due to the electrostatic repulsion. The percentage removal of IC increases with increasing temperature, suggesting that the IC adsorption onto AC is an endothermic process. The thermodynamic study for the adsorption shows that the process is spontaneous and endothermic in nature. The adsorption data obtained under equilibrium conditions can be fitted well by the Langmuir isotherm model. The adsorption kinetics is discussed by the pseudo-second-order kinetic and intraparticle diffusion models. It is found that the adsorption well follows the pseudo-second-order kinetic model for all studied concentrations. Desorption studies suggested that the adsorption process was not reversible under some circumstances. This study suggests that the AC prepared from PS exhibits good adsorption properties and can be used for the removal of IC from wastewater as a low-cost adsorbent.

Acknowledgments

The authors are grateful for the financial support by the Nature Science Foundation of Hebei Province (No. B2012408006), the Nature Science Foundation of Langfang Teachers' college (No. LSZZ201304).

Nomenclature

- C_i — initial concentrations of IC solution (mg/L)
- C_e — equilibrium concentrations of IC solution (mg/L)
- V — volume of IC solution (L)
- W — mass of the adsorbent (g)
- K_c — equilibrium constant
- C_{Ae} — mass of IC adsorbed onto AC per liter of the solution at equilibrium (mg/L)
- ΔG° — change of Gibbs free energy (kJ/mol)
- ΔH° — change of enthalpy (kJ/mol)
- ΔS° — change of entropy (J/mol K)
- R — gas constant (8.314 J/mol K)
- T — absolute temperature (K)
- K_L — Langmuir constants (L/mg)
- q_m — maximum adsorption capacity (mg/g)
- R_L — dimensionless equilibrium parameter
- q_t — amount of dye adsorbed at a time t (mg/g)
- k_2 — rate constant of pseudo-second-order (g/mg min)
- K_i — rate constant of intraparticle diffusion (mg/g min^{0.5})
- C_i — the thickness of the boundary layer

References

- [1] S. You, S. Cheng, H. Yan, The impact of textile industry on China's environment, *Int. J. Fashion Des., Technol. Educ.* 2 (2009) 33–43.
- [2] J.A. Rauh-Hain, M.R. Laufer, Increased diagnostic accuracy of laparoscopy in endometriosis using indigo

- carmin: A new technique, *Fertil. Steril.* 95 (2011) 1113–1114.
- [3] A. Mittal, J. Mittal, L. Kurup, Batch & bulk removal of hazardous dye, indigo carmine from wastewater through adsorption, *J. Hazard. Mater.* 137 (2006) 591–602.
- [4] M.M. Sari, Removal of acidic indigo carmine textile dye from aqueous solutions using radiation induced cationic hydrogels, *Water Sci. Technol.* 61 (2010) 2097–2104.
- [5] M. Dalaran, S. Emik, G. Güçlü, T.B. İyim, S. Özgümüş, Study on a novel polyampholyte nanocomposite superabsorbent hydrogels: Synthesis, characterization and investigation of removal of indigo carmine from aqueous solution, *Desalination* 279 (2011) 170–182.
- [6] O. Türgay, G. Ersöz, S. Atalay, J. Forss, U. Welander, The treatment of azo dyes found in textile industry wastewater by anaerobic biological method and chemical oxidation, *Sep. Purif. Technol.* 79 (2011) 26–33.
- [7] S.S. Moghaddam, M.R. Moghaddam, M. Arami, Coagulation/flocculation process for dye removal using sludge from water treatment plant: Optimization through response surface methodology, *J. Hazard. Mater.* 175 (2010) 651–657.
- [8] A.Y. Zahrim, C. Tizaoui, N. Hilal, Removal of highly concentrated industrial grade leather dye: Study on several flocculation and sand filtration parameters, *Sep. Sci. Technol.* 46 (2011) 883–892.
- [9] P.S. Zhong, N. Widjojo, T. Chung, M. Weber, C. Maletzko, Positively charged nanofiltration (NF) membranes via UV grafting on sulfonated polyphenylenesulfone (sPPSU) for effective removal of textile dyes from wastewater, *J. Membr. Sci.* 417–418 (2012) 52–60.
- [10] P. Liao, Z.M. Ismael, W. Zhang, S. Yuan, M. Tong, K. Wang, J. Bao, Adsorption of dyes from aqueous solutions by microwave modified bamboo charcoal, *Chem. Eng. J.* 195–196 (2012) 339–346.
- [11] H.M.H. Gad, A.A. El-Sayed, Activated carbon from agricultural by-products for the removal of Rhodamine-B from aqueous solution, *J. Hazard. Mater.* 168 (2009) 1070–1081.
- [12] L.W. Low, T.T. Teng, A.F.M. Alkarkhi, A. Ahmad, N. Morad, Optimization of the adsorption conditions for the decolorization and COD reduction of methylene blue aqueous solution using low-cost adsorbent, *Water Air Soil Pollut.* 214 (2011) 185–195.
- [13] M.A.M. Salleh, D.K. Mahmoud, W.A.W.A. Karim, A. Idris, Cationic and anionic dye adsorption by agricultural solid wastes: A comprehensive review, *Desalination* 280 (2011) 1–13.
- [14] Y. Wang, W. Chu, Adsorption and removal of a xanthene dye from aqueous solution using two solid wastes as adsorbents, *Ind. Eng. Chem. Res.* 50 (2011) 8734–8741.
- [15] M. Asgher, H.N. Bhatti, Evaluation of thermodynamics and effect of chemical treatments on sorption potential of Citrus waste biomass for removal of anionic dyes from aqueous solutions, *Ecol. Eng.* 38 (2012) 79–85.
- [16] M.S. Rehman, I. Kim, J.I. Han, Adsorption of methylene blue dye from aqueous solution by sugar extracted spent rice biomass, *Carbohydr. Polym.* 90 (2012) 1314–1322.
- [17] M.C. Shih, Kinetics of the batch adsorption of methylene blue from aqueous solutions onto rice husk: Effect of acid-modified process and dye concentration, *Desalin. Water Treat.* 37 (2012) 200–214.
- [18] L.C. Romero, A. Bonomo, E.E. Gonzo, Acid-activated carbons from peanut shells: Synthesis, characterization and uptake of organic compounds from aqueous solutions, *Adsorpt. Sci. Technol.* 21 (2003) 617–626.
- [19] Z.A. AL-Othman, R. Ali, M. Naushad, Hexavalent chromium removal from aqueous medium by activated carbon prepared from peanut shell: Adsorption kinetics, equilibrium and thermodynamic studies, *Chem. Eng. J.* 184 (2012) 238–247.
- [20] K.Y. Foo, B.H. Hameed, Preparation of activated carbon from date stones by microwave induced chemical activation: Application for methylene blue adsorption, *Chem. Eng. J.* 170 (2011) 338–341.
- [21] A.V. Maldhure, J.D. Ekhe, Microwave treated activated carbon from industrial waste lignin for endosulfan adsorption, *J. Chem. Technol. Biotechnol.* 86 (2011) 1074–1080.
- [22] W. Plazinski, W. Rudzinski, A. Plazinska, Theoretical models of sorption kinetics including a surface reaction mechanism: A review, *Adv. Colloid Interface Sci.* 152 (2009) 2–13.
- [23] Y. Wang, E.J. Reardon, Activation and regeneration of a soil sorbent for defluoridation of drinking water, *Appl. Geochem.* 16 (2001) 531–539.
- [24] G. Sreelatha, V. Ageetha, J. Parmar, P. Padmaja, Equilibrium and kinetic studies on reactive dye adsorption using palm shell powder (an agrowaste) and chitosan, *J. Chem. Eng. Data* 56 (2011) 35–42.
- [25] V. Vadivelan, K.V. Kumar, Equilibrium, kinetics, mechanism, and process design for the sorption of methylene blue onto rice husk, *J. Colloid Interface Sci.* 286 (2005) 90–100.
- [26] C.M. Ghimbeu, R. Gadiou, J. Dentzer, L. Vidal, C. Vix-Guterl, A TPD-MS study of the adsorption of ethanol/cyclohexane mixture on activated carbons, *Adsorption* 17 (2011) 227–233.